Journal of Physics: Conference Series **1643** (2020) 012148 doi:10.1088/1742-6596/1643/1/012148

Investigation of the Pygmy Dipole Resonance in photon scattering experiments

Miriam Müscher[1], Johann Isaak[2], Deniz Savran[3], Ronald Schwengner[4], Julius Wilhelmy[1] and Andreas Zilges[1]

[1] Universität zu Köln, Institut für Kernphysik, Zülpicher Str. 77, 50937 Köln, Germany
[2] Institut für Kernphysik, Technische Universität Darmstadt, Schlossgartenstr. 9, 64289 Darmstadt, Germany
[3] GSI Helmholtzzentrum für Schwerionenforschung GmbH, Planckstr. 1, 64291 Darmstadt, Germany
[4] Institut für Strahlenphysik, Helmholtz-Zentrum Dresden-Rossendorf, Bautzner Landstr. 400, 01328 Dresden, Germany

E-mail: muescher@ikp.uni-koeln.de

Abstract. The Pygmy Dipole Resonance (PDR) is the dominating electric dipole excitation below and around the particle separation threshold and exhausts only a few percent of the energy-weighted sum rule. Nevertheless, it may have some impact on reaction rates in nucleosynthesis processes. Therefore, investigations to get more insights in this excitation mode are crucial. A common approach to study the PDR of atomic nuclei is the Nuclear Resonance Fluorescence method (NRF) which bases on real-photon scattering. Absolute cross sections, spin and parity quantum numbers are determined in a model-independent way if suited experimental setups are used. In general, there are two complementary NRF experiments which are presented in this paper.

1. Introduction

The Pygmy Dipole Resonance (PDR) is an electric dipole excitation on top of the low-energy tail of the Isovector Giant Dipole Resonance (IVGDR) [1]. Despite its relatively low proportion to the energy-weighted sum rule (EWSR), some theoretical calculations predict a huge impact on, e.g., reaction rates of the rapid neutron-capture process (r process) [2, 3]. This process is responsible for about half of the abundances of nuclei heavier than iron in our universe and precise knowledge about the reaction rates may help to deepen the understanding of nucleosynthesis. Besides the uncertainty about the effect of the PDR on nucleosynthesis, the collectivity of the PDR is still under debate. Some theories interpret it in a macroscopic picture as an oscillation of an isospin-saturated core against a neutron skin whereas other theories predict that the origin of the enhanced cross sections is due to single-particle excitations (see Ref. [1] and references therein). To provide greater clarity about the structure of the PDR experimental and theoretical studies of the dipole response in this energy region are important.
Real-photon scattering is often used for this purpose and the method is described in the following.

2. Method

The Nuclear Resonance Fluorescence (NRF) method is a commonly used approach to study the low-lying dipole response in atomic nuclei [4]. The technique is especially suited for this purpose due to its selectivity for the predominant excitation of nuclear states by dipole radiation and with a lower probability by quadrupole radiation. Real photons excite atomic nuclei from the ground state J_0^π to an excited state J^π (see black arrow in Fig. 1). The subsequently emitted photons of the de-excitation are investigated. In general, there are two possibilities for the de-excitation. The first is called an elastic transition and is shown in Fig. 1 by the green arrow. In this case, the emitted photon has the same energy as the γ ray in the entrance channel. The second possibility is called an inelastic transition which means that the de-excitation is via lower-lying but still excited states (see red arrows in Fig. 1).

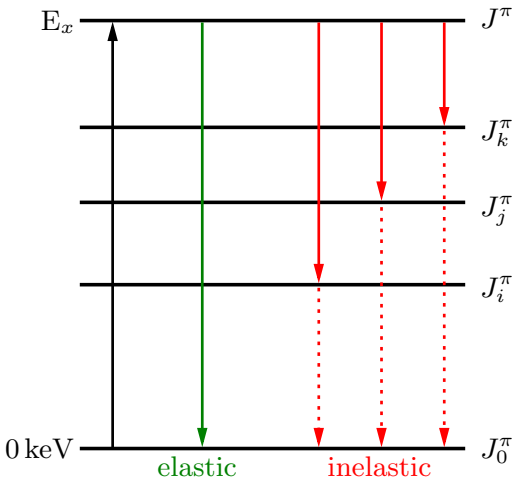

Figure 1. The principle of the NRF technique is shown. The nucleus is excited from its ground state J_0^π to an excited state J^π by the absorption of a γ quantum (black upward arrow). The de-excitation can occur in several ways which are indicated by the downward arrows. The green arrow illustrates the direct decay back to the ground state which is called elastic transition and the red arrows indicate inelastic decays via intermediate states. In addition, the spin and parity quantum numbers of the states are given J_n^π.

NRF experiments enable the extraction of energy-integrated cross sections I_S of excited states by using Eq. (1).

$$I_S = \frac{A}{N_T \cdot W(\theta) \cdot \epsilon(E_\gamma) \cdot N_\gamma(E_\gamma)} \tag{1}$$

Here, A equals the peak volume in the de-excitation spectra, N_T is the number of target nuclei and $W(\theta)$ the angular distribution of the emitted radiation at the observation angle θ. $\epsilon(E_\gamma)$ denotes the full-energy peak efficiency which is determined by source measurements and simulations. The number of photons hitting the target of interest per energy and per area $N_\gamma(E_\gamma)$ is more difficult to determine and different techniques are used depending on the photon source. The most common method is described in the corresponding parts of Sec. 3.

3. NRF experiments with different photon sources

There are two main photon sources which are used for the generation of photon beams. In the following both techniques are presented.

3.1. Bremsstrahlung

Bremsstrahlung is generated by accelerated electrons which impinge on a radiator target. There, the electrons are slowed down or stopped by the interaction with the Coulomb field of the radiator nuclei. In this way, part of the electrons' kinetic energy is converted into electromagnetic radiation generating a continuous photon flux whereby the endpoint energy of the photon flux

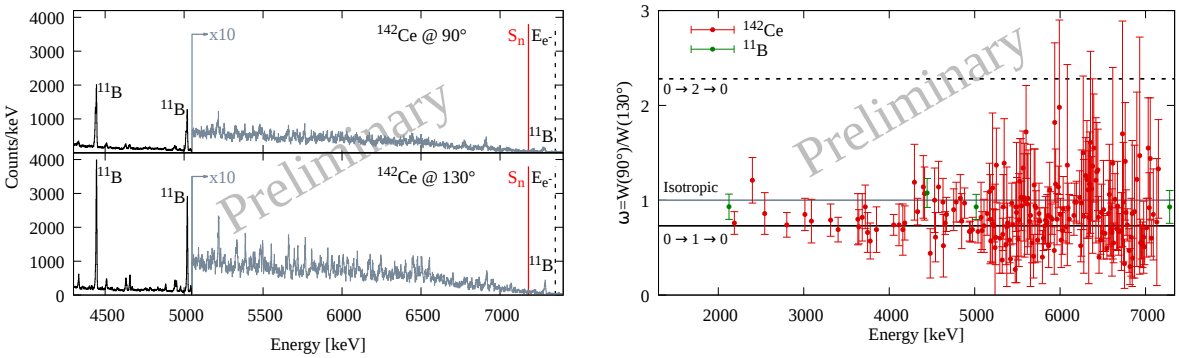

Figure 2. *Left:* De-excitation spectra of ^{142}Ce for scattering angles of $\theta = 90°$ (upper part) and $\theta = 130°$ (lower part) which was measured at DHIPS with an endpoint energy of $E_{e^-} = 7.35\,\text{MeV}$ (black dashed line). The neutron separation threshold of ^{142}Ce is $S_n = 7.17\,\text{MeV}$ and is indicated by the red line. Transitions of the calibration standard ^{11}B are marked. Above $E \approx 5050\,\text{keV}$ the spectra are multiplied by 10 (gray spectra). *Right:* The intensity ratios between $\theta = 90°$ and $\theta = 130°$ of ^{142}Ce (red dots) and of the calibration standard ^{11}B (green dots) are displayed. The latter ones are close to unity (gray line) due to the non-zero ground-state spin of ^{11}B. For an even-even nucleus, the expected value of a dipole transition equals $\omega_{theo}(\text{dipole}) = 0.73$ (solid black line) and of a quadrupole de-excitation $\omega_{theo}(\text{quadrupole}) = 2.28$ (dashed black line).

distribution is reached by fully stopped electrons.

The continuous photon flux enables the investigation of many transitions in the chosen energy range in a single experiment. The left part of Fig. 2 illustrates the bremsstrahlung de-excitation spectra of ^{142}Ce which was measured at the Darmstadt High-Intensity Photon Setup (DHIPS) [5]. The endpoint energy was $E_{e^-} = 7.35\,\text{MeV}$ (black dashed line) which is about 200 keV higher than the neutron separation threshold of ^{142}Ce $S_n = 7.17\,\text{MeV}$ (red line). In addition to the target of interest, ^{11}B was used as calibration standard and its transitions are marked in Fig. 2. Using detectors at different scattering angles θ relative to the beam axis allows the distinction of multipolarities of the observed de-excitations due to different angular distributions of dipole and quadrupole transitions. For this purpose scattering angles of $\theta \approx 90°$ and $\theta \approx 130°$ are most suited because the difference between the ratios of the distributions for $L = 1$ and $L = 2$ is largest. The intensity ratios ω between the detector positions can be calculated via:

$$\omega = \frac{A(90°)}{A(130°)} \cdot \frac{\epsilon(130°)\tau(130°)}{\epsilon(90°)\tau(90°)} \tag{2}$$

where τ denotes the dead time correction of the detectors. If this value is close to $\omega = 0.73$ ($\omega = 2.28$) a dipole (quadrupole) transition is observed. The intensity ratios of the ^{142}Ce experiment are displayed in the right part of Fig. 2.

The ^{11}B calibration standard can be used for the determination of the absolute photon flux which enables the extraction of absolute photon absorption cross sections of the target nucleus. By performing simulations of the bremsstrahlung-production process, the shape of the γ-ray distribution can be determined but the exact number of γ quanta impinging on the target is difficult to obtain. Therefore, the relative photon flux is scaled to well-known transitions of the calibration standard. To minimize systematic uncertainties it is established to use the product of photon flux and detection efficiency which is illustrated in Fig. 3.

Besides DHIPS, Bremsstrahlung is also used at the γELBE facility at the Helmholtz-Zentrum Dresden-Rossendorf (HZDR) to investigate the dipole response of atomic nuclei [6].

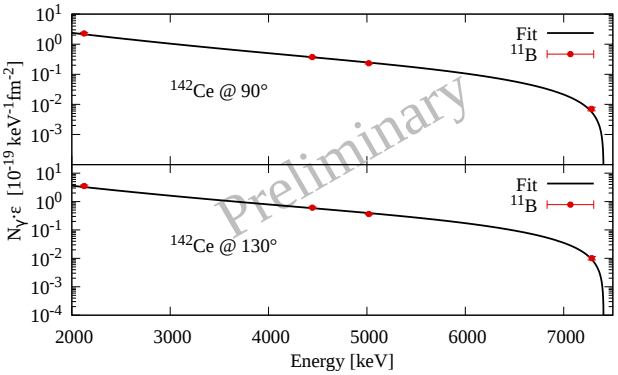

Figure 3. The figure illustrates the determined shapes of the product of photon flux N_γ and the detection efficiencies ϵ for both scattering angles in dependence on the γ-ray energy. These shapes (black) are scaled to the values deduced for known transitions in the calibration standard ^{11}B (red dots).

3.2. Laser-Compton Backscattering

The Laser-Compton Backscattering (LCB) technique bases on Compton scattering of laser photons in the eV range on ultra-relativistic electrons (MeV−GeV). Thereby, the photons experience an energy boost which is the greatest if the incidence angle is close to 180°. The resulting γ rays are quasi-monoenergetic and reach energies in the MeV range. Due to the fact that Compton scattering conserves the polarization a linearly polarized γ-ray beam is generated if the laser beam is polarized. This enables the assignment of parity quantum numbers to excited states if detectors are placed at different polar angles, preferentially, parallel and perpendicular relative to the polarization plane.

The LCB technique is used as photon source, e.g., at the High Intensity γ-ray Source (HIγS) at the Triangle Universities Nuclear Laboratory (TUNL) and Duke University [7], at the NewSUBARU setup at the University of Hyogo, Japan, [8] and will be used at the upcoming facility ELI-NP which is currently under construction in Romania [9].

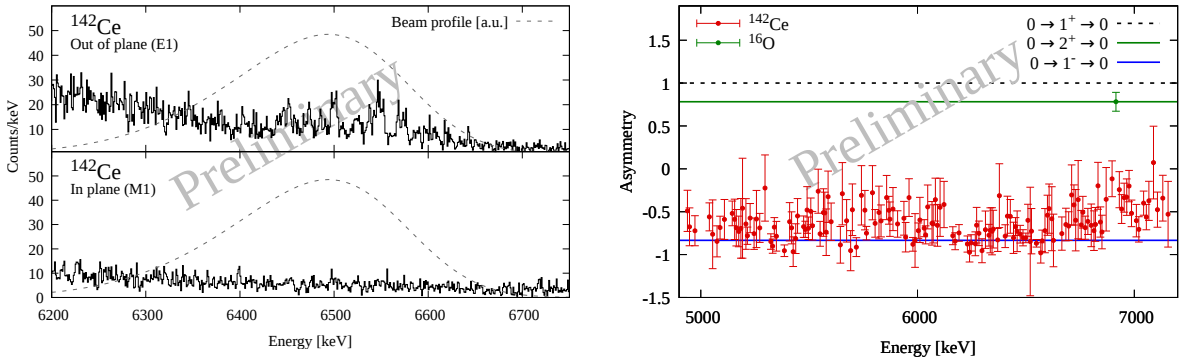

Figure 4. *Left:* The de-excitation spectrum of ^{142}Ce of the detector perpendicular (parallel) to the polarization plane is displayed in the upper (lower) part for a beam energy of 6.5 MeV. The dashed lines mark the beam profile in arbitrary units. *Right:* The extracted asymmetry values of all observed transitions in ^{142}Ce (red points) and the decay of the 2_1^+ state of ^{16}O (green points) are shown. In addition, the averaged asymmetries for electric dipole (blue) and electric quadrupole transitions (green) and the expected value of a magnetic dipole transition (black dashed) are indicated by horizontal lines.

The left part of Fig. 4 depicts the de-excitation spectra of ^{142}Ce for the above named detector positions for a beam energy of 6.5 MeV which was measured at HIγS. The clear difference between $E1$ and $M1$ transitions for even-even nuclides is obvious and enables firm parity quantum number assignments to the corresponding nuclear states. Quantitatively, the dipole

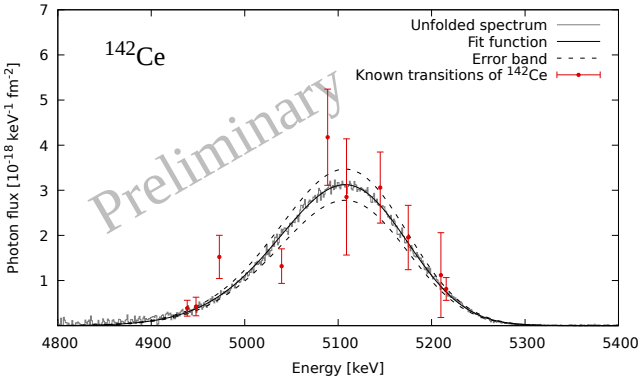

Figure 5. An unfolded spectrum of the flux monitor (gray) is shown in dependence on the γ-ray energy for a beam energy of 5.1 MeV of the NRF experiment on ^{142}Ce at HIγS. The black line is the fit function which was scaled to already known transitions of ^{142}Ce (red points) studied in a bremsstrahlung experiment.

character assignment can be performed by calculating the so-called asymmetry ϵ via:

$$\epsilon = \frac{N_{\parallel,cor} - N_{\perp,cor}}{N_{\parallel,cor} + N_{\perp,cor}} \approx \begin{cases} +1 & \text{magnetic transition} \\ -1 & \text{electric transition} \end{cases} \tag{3}$$

$N_{\perp,cor}$ and $N_{\parallel,cor}$ are the numbers of detected events corrected by the corresponding detection efficiencies and system's live times of the detectors perpendicular and parallel to the polarization plane, respectively. The right part of Fig. 4 shows the extracted asymmetry values of ^{142}Ce (red points) whereby most asymmetries are close to -1 and, therefore, most of the de-excitations can be characterized as electric dipole transitions. The asymmetry values are not exactly -1 because of, e.g., the finite opening angles of the detectors. Additionally, the asymmetry of the ground-state transition of the 2_1^+ state of ^{16}O is indicated by the green dot close to $+1$ which is expected for an electric quadrupole transition.

For the photon flux determination a movable 123 % HPGe detector is used at HIγS which can be placed in the beam line for each beam-energy setting. Due to the high number of photons ($\approx 10^7 \frac{1}{\mathrm{s}}$), the γ beam is reduced by attenuators which is the reason why the absolute photon flux cannot be directly measured. The recorded spectra have to be deconvoluted by using the detector response, which is simulated. A resulting beam profile is depicted in the left part of Fig. 4 in arbitrary units by the dashed line and in Fig. 5 by the gray spectrum. The absolute photon flux determination can be performed by scaling the shape of the photon flux to already known transitions of the target itself. Due to this, bremsstrahlung experiments are indispensable for the determination of absolute cross sections in LCB measurements. This method is illustrated in Fig. 5 for a beam energy of 5.1 MeV of the ^{142}Ce experiment.

The use of a quasi-monoenergetic photon source enables a clear distinction of elastic and inelastic decay channels because all transitions which appear below the excitation-energy range stem from inelastic transitions. The experiment on ^{142}Ce was performed at the parasitic setup at HIγS and in comparison to the γ^3 setup [10] only two HPGe detectors were positioned at a scattering angle of $\theta = 90°$, one parallel and one perpendicular to the polarization plane. Therefore, γ-γ-coincidences could not be applied but averaged inelastic cross sections were extracted [11]. For this purpose, the decay of the 2_1^+ state is well-suited because most of the energetically low-lying states, which might be previously fed by excited states, decay themselves via the 2_1^+ state. In this way this state acts like a funnel and its decay serves as good estimation for the amount of inelastic decays [11]. Hence, the averaged inelastic cross section can be determined with

$$\sigma_{\gamma\gamma'} = \frac{A(2_1^+)}{N_T \cdot \hat{W} \cdot \epsilon(E_{2_1^+}) \cdot \int_0^\infty N_\gamma dE_\gamma} \tag{4}$$

where the quantities have the same meaning as in Sec. 2 just regarding the 2_1^+ state. $\hat{W}$ is an averaged angular distribution which is approximated by 1 because a distinction between different

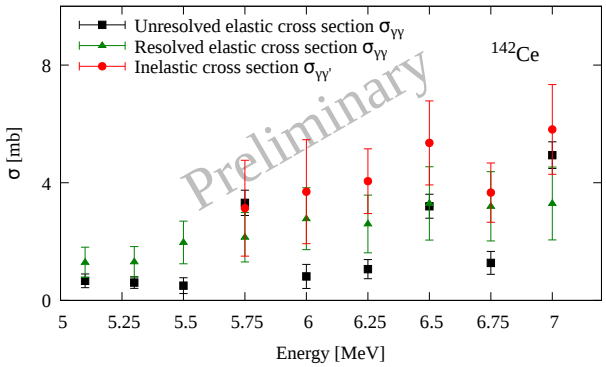

Figure 6. The different contributions to the total photon absorption cross section are illustrated. The elastic cross section can be divided into unresolved (black squares) and resolved strength (green triangles). The amount of inelastic decays is estimated by the decay of the 2_1^+ state and the corresponding cross sections are illustrated by the red circles.

decay cascades is not possible. $\int_0^\infty N_\gamma dE_\gamma$ denotes the integral of the photon flux over the whole energy range. The contributions of the inelastic cross section are illustrated in Fig. 6 by the red dots and it can be seen that this part of the cross section is of utmost importance.
A further component to the total photon-absorption cross section is strength that cannot be resolved in a state-to-state analysis because the transitions are too weak and are hidden in the continuum of the spectrum (unresolved strength). In bremsstrahlung measurements unresolved strength cannot be experimentally investigated due to the bremsstrahlung background which does not occur at LCB facilities. Unfortunately, there was no vacuum in the beam pipe during the ^{142}Ce experiment at HIγS. For this reason, there is some background on the low-energy side of the spectrum (cf. left part of Fig. 2) which has to be subtracted before investigating the unresolved strength. After the subtraction, the resulting spectra contain only the elastic part of strength within the excitation region. By using the investigated transitions of the state-to-state analysis (resolved strength), the contribution of unresolved strength can be extracted. Fig. 6 illustrates the resolved (green triangles) and the unresolved elastic cross sections (black squares). The figure highlights the importance to study each component of photon absorption cross section.

4. Conclusion

The Nuclear Resonance Fluorescence technique and its advantages for the investigation of dipole excitations are presented. The two common kinds of NRF experiments are described and some analysis steps are explained with the help of $(\gamma\gamma')$ experiments on ^{142}Ce. On the one hand, bremsstrahlung measurements are important to determine absolute cross sections and, on the other hand, LCB experiments are indispensable to extract total photon absorption cross sections. The importance of both complementary experiments is outlined.

Acknowledgments

This work is supported by the BMBF under grant 05P18PKEN9.

References

[1] Savran D, Aumann T and Zilges A 2013 *Prog. Part. Nucl. Phys.* **70** 210
[2] Goriely S 1998 *Phys. Lett.* B **436** 10
[3] Litvinova E *et al.* 2009 *Nucl. Phys.* A **823** 26
[4] Kneissl U, Pitz H H and Zilges A 1996 *Prog. Part. Nucl. Phys.* **37** 349
[5] Sonnabend K *et al.* 2011 *Nucl. Instr. and Meth.* A **640** 6-12
[6] Schwengner R *et al.* 2005 *Nucl. Instr. and Meth.* A **555** 211
[7] Weller H R *et al.* 2009 *Prog. Part. Nucl. Phys.* **62** 257-303
[8] Miyamoto S *et al.* 2006 *Radiat. Meas.* **41** S179-S185
[9] Ur C A *et al.* 2016 *Rom. Rep. Phys.* **68** S483
[10] Löher B *et al.* 2013 *Nucl. Instr. and Meth.* A **723** 136
[11] Tonchev A P *et al.* 2010 *Phys. Rev. Lett.* **104** 072501